

Multimodal Microstructural and Cellular Assessment of Magnesium Phosphate Cement in Rat Unicortical Diaphyseal Defect Healing

Nithin Sankar S¹, Francis B. Fernandez², Dinesh P T³, Jinesh Kumar N.S.⁴, Remya V⁴, Hamza Palekkodan⁵

Department of Veterinary Surgery & Radiology

Kerala Veterinary & Animal Sciences University, Pookode

Affiliations

1. PG Scholar
2. Scientist C, Division of Bio-ceramics, BMT Wing, SCTIMST
3. Associate Professor & Head
4. Assistant Professor
5. Assistant Professor, Dept. of Pathology

Corresponding Author: Dinesh P T, e – mail – dineshpt@kvasu.ac.in,

ABSTRACT

Background:

Magnesium phosphate cement (MPC) has emerged as a promising bone substitute due to its rapid setting, biocompatibility, controlled degradation, and favourable osteoconductive characteristics. However, comprehensive in vivo evaluations that integrate radiographic, histological, histomorphometric, and microstructural analyses in diaphyseal cortical defects remain scarce.

Objective:

This study aimed to investigate the healing dynamics of a standardised unicortical femoral diaphyseal defect in rats treated with MPC, using a multimodal evaluation strategy to characterise inflammatory response, osteoid formation, vascularisation, defect bridging, and biomaterial resorption.

Materials and Methods:

A total of 21 adult male Wistar rats underwent surgically created 2×6 mm unicortical femoral defects, filled with MPC. Animals were monitored for 2, 6, and 12 weeks. Healing progression was evaluated by histopathology, histomorphometry, and scanning electron microscopy (SEM).

Results:

Histologically, early phases were characterised by inflammatory infiltration and limited woven bone; by week 6, trabecular networks had expanded with coexisting woven and lamellar bone. By week 12, mature lamellar bone predominated, with reduced fibrosis and improved cortical continuity. Histomorphometry confirmed progressive decreases in inflammation and vascularity and increased osteoid deposition. SEM revealed early interfacial gaps that gradually consolidated into organised lamellar-like structures with visible mineralisation fronts.

Conclusion:

MPC demonstrated favourable biocompatibility, osteoconductive behaviour, and controlled biodegradation over the 12-week healing period. While remodelling remained incomplete in some regions, the cement supported progressive bone infill, stable integration, and gradual replacement with organised bone matrix. The findings highlight MPC as a bone graft substitute for small to moderate cortical defects and support its further optimisation for higher load-bearing applications.

Keywords: magnesium phosphate cement, bone regeneration, histomorphometry, SEM, diaphyseal defect, rat model, biomaterials

1. INTRODUCTION

The restoration of bone continuity following traumatic, neoplastic, or pathological defects remains a significant challenge in orthopaedic and reconstructive surgery (Roberts & Rosenbaum, 2012). Although autologous bone grafting is considered the gold standard, its clinical utility is constrained by donor site morbidity, limited graft volume, and increased operative complexity. These limitations have stimulated growing interest in synthetic, biocompatible, and bioactive substitutes capable of promoting osteoconduction, osteoinduction, and long-term osseointegration. Within this context, bone cements have emerged as valuable alternatives due to their ease of shaping, defect conformability, and suitability for complex anatomical sites.

Polymethyl methacrylate (PMMA) was historically the most widely used cement; however, issues such as excessive heat generation during curing, cytotoxicity, and non-degradability have restricted its current use. Calcium phosphate cement (CPC) was later introduced with improved biocompatibility and resorbability, yet its application remains limited by insufficient mechanical strength and modest neurogenic capability. Magnesium phosphate cement (MPC) has since drawn considerable attention as a next-generation material due to its rapid setting, high early compressive strength, controlled degradability, and favourable biological interactions. Tian et al. (2024) reported that MPC exhibits superior compressive strength and a desirable resorption profile, while in vitro studies have demonstrated enhanced osteoblastic proliferation and mineral deposition mediated by magnesium ion release and apatite layer formation, as noted by Gelli and Ridi (2023). The authors further emphasized the potential of incorporating additional bioactive phases to optimise the mechanical and biological properties of MPC.

This study initiates the evaluation of MPC for the restoration of unicortical diaphyseal defect in the rat models.

2. MATERIALS AND METHODS

Ethical Approval and Study Design

This controlled experimental study was conducted on 21 adult male Wistar rats (8 weeks old, 150–200 g body weight), procured from a CCSEA-approved laboratory animal facility at the College of Veterinary and Animal Sciences, Pookode. All procedures adhered to CCSEA guidelines, and ethical approval was obtained from the Institutional Animal Ethics Committee (IAEC/COVAS/PKD/22/2/2024).

Each animal underwent creation of bilateral unicortical diaphyseal femoral defects (2 mm × 6 mm). The left femur received magnesium phosphate cement (MPC, control), and the right femur received the MP-HASi composite cement (test). Biomaterials were provided by the Bioceramics Laboratory, SCTIMST, Thiruvananthapuram. Animals were observed for 12 weeks postoperatively for radiographic, morphological, histologic, and SEM-based evaluation.

Preparation of Bone Cements

Magnesium phosphate cements (MPC) were prepared immediately before implantation by mixing the powdered component with the solvent to obtain a uniform pasty consistency, as per laboratory specifications.

Preoperative Preparation

Animals were randomly selected and fasted for one hour prior to anaesthesia. The hindlimb was shaved, washed with soap and water, degreased with 70% alcohol, and disinfected using povidone-iodine. All rats received 2 mL normal saline intraperitoneally, 30 minutes before induction.

Anaesthesia and Surgical Procedure

Anaesthesia

Premedication consisted of buprenorphine (0.05 mg/kg SC). Anaesthesia was induced using a combination of xylazine (3 mg/kg IP) and ketamine (30 mg/kg IP), following IACUC guidelines. A stock anaesthetic mixture (xylazine 100 mg/mL and ketamine 50 mg/mL) diluted to 20 mL was administered at 0.1 mL/100 g body weight. Anaesthesia was maintained with isoflurane (1–2% in oxygen).

Surgical Approach

The lateral approach to the femur described by Costa et al. (2011) was used. A linear incision was made along the lateral thigh, and the intermuscular plane between the superficial gluteus and biceps femoris was bluntly dissected to expose the diaphysis. All muscular attachments were gently elevated, and the femoral shaft was isolated. A standardized unicortical defect (2 mm × 6 mm) was created using a 2 mm dental bur. Defects were filled with MPC cement accordingly. Following cement setting, muscle layers and skin were closed with polyamide 3-0 in a simple continuous pattern.

Postoperative Care

Postoperative management included ceftriaxone (40 mg/kg IM, twice daily for 7 days) and meloxicam (2 mg/kg SC for 5 days). Wounds were dressed twice daily with povidone-iodine ointment. Skin sutures were removed on postoperative day 10. Animals were monitored daily for complications.

Euthanasia and Sample Collection

At predetermined time points (2, 6, and 12 weeks), femurs were harvested for evaluation. Euthanasia was performed using an intraperitoneal overdose of 5% thiopentone sodium in accordance with CCSEA guidelines.

4. RESULT

The experiment was carried out on 21 adult male Wistar rats, each weighing approximately 250 g. Defects were created in both femurs, designated as the control and test groups. Standardised unicortical diaphyseal defects measuring 2×6 mm were produced in each femur. The control defects in the left femur were treated with magnesium phosphate cement (MPC). In contrast the test defects in the right femur were treated with magnesium phosphate–hydroxyapatite–silica (MP-HASI) composite cement.

4.1. SELECTION AND EVALUATION OF EXPERIMENTAL ANIMALS

The rats used in the study were sourced from the Lab Animal Facility, CVAS, Pookode and selected randomly. All animals tolerated the treatment protocol well. The surgical incisions healed without any complications. Skin sutures were removed on the 10th post-operative day after complete healing of the skin wound.

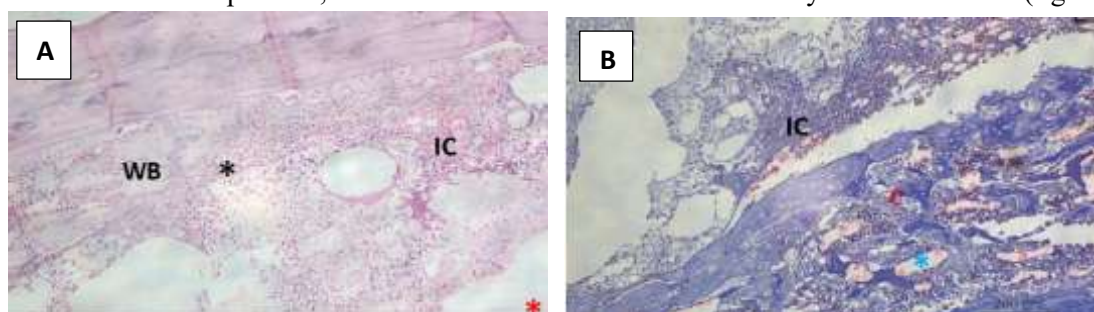
HISTOPATHOLOGICAL EVALUATION

Harvested healed segments of bone were decalcified, sectioned and stained using haematoxylin and eosin and Masson's Trichrome stain, which were evaluated microscopically.

At two weeks post-implantation, the group exhibited remnants of the graft material, appearing as pink amorphous material under haematoxylin and eosin staining.

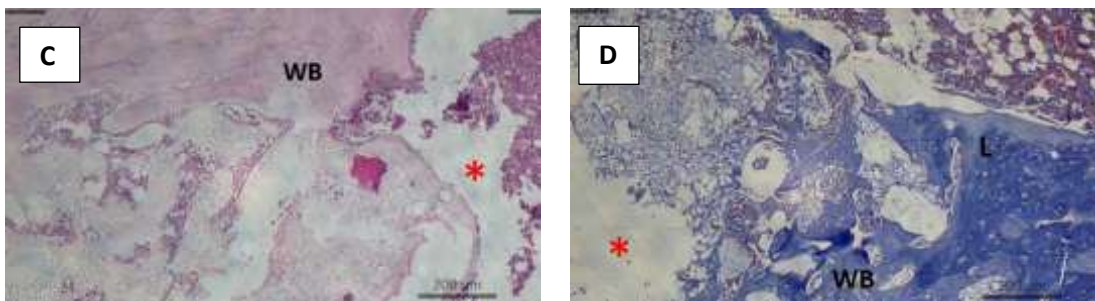
The MPC group showed a defect gap, inflammatory cell infiltration, prominent fibrous callus formation, and initiates woven bone development, restricted to early extensions from the cortical margins (figure A).

Masson's trichrome-stained sections supported these observations; in the present group, dense blue-stained fibrous tissue with woven bone deposition, numerous blood vessels and inflammatory cells was evident (figure B).



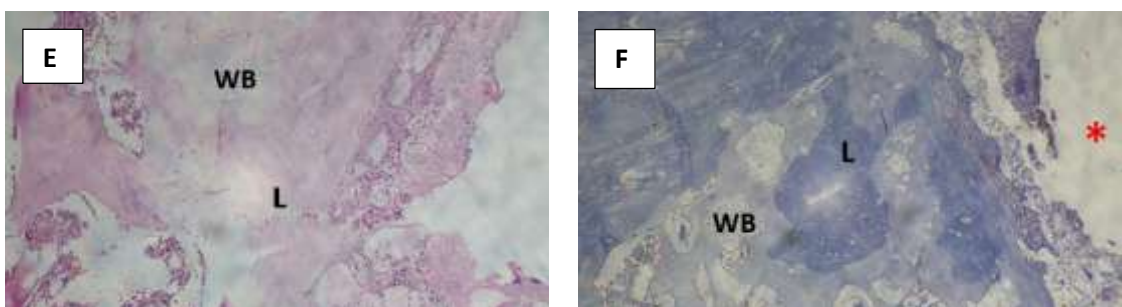
A. Fibrous callus (*) deposition around the defect area (x10, H & E), inflammatory cells (IC), woven bone and clearly visible defect area (*). **B.** Well organised collagen deposition (C) in defect site (x10, Mason's Trichrome) with vascularization (*) and inflammatory cells (IC).

By six weeks, signs of graft integration and bone remodelling were evident in the group. In the group, the graft material was well integrated with minimal inflammatory infiltration. The newly formed bone appeared thicker and more organised. However, remnants of the graft material remained in the central region of the defect (figure C). Masson's trichrome staining revealed islands of newly formed bone as light blue areas interspersed with focal dark blue staining, denoting localised maturation within the regions of active bone formation (figure D).



C. Defect (*) filled by sheets of woven bone (WB) (x10, H & E). **D.** Lamellar (* bright blue colour) with collagen deposition and woven bone (light blue colour) at defect site (*) (x10, Mason's Trichrome).

By twelve weeks, the group demonstrated advanced stages of bone healing, though the extent of maturation varied. In the control group, partial bridging of the defect edges, with a visible central gap, was observed. The presence of both woven and lamellar bone indicated ongoing maturation, and the newly formed bone was well integrated with the host tissue. However, a thin fibrous capsule separated the new bone from the remaining central gap. Corresponding Masson's trichrome staining showed darker-stained new bone at the centre, gradually transitioning to lighter blue areas toward the periphery, reflecting varying degrees of mineralisation.



E. Diffused zone of lamellar bone with decreased amount of woven bone (WB) (x10, H & E). **F.** Lamellar bone (bright blue colour) with small amount of woven bone (WB) (appeared as light blue) with defect gap (*) (x10, Mason's Trichrome). D-defect

Histomorphometry

Histomorphometric evaluation was performed by counting cell types in five randomly selected fields at the defect site on each slide. Each feature—*viz.* the level of inflammation, neovascularisation, fibrosis, the type and amount of new bone formed, and the degree of edge bone integration—was assessed and scored accordingly (Table 1.).

Table 1 Histomorphometry observations

Parameter	MPC		
	2 nd Week	5 th Week	12 th Week
Inflammation	0.60 ± 0.24^a	2.40 ± 0.24	2.60 ± 0.24
Vascularity	3.00 ± 0.00	1.50 ± 0.32	0.20 ± 0.20
Fibrosis	1.40 ± 0.4	1.40 ± 0.00	2.10 ± 0.24
New Bone Type	0.20 ± 0.2	0.40 ± 0.24	2.00 ± 0.32
New Bone Quantity	0.40 ± 0.4	0.80 ± 0.49	2.00 ± 0.00
Host bone integration	1.40 ± 0.6	2.40 ± 0.24	3.00 ± 0.00
Total	7.00 ± 0.42	8.9 ± 0.43	11.9 ± 0.41

4.4.1.1.

Inflammation

At two weeks, the group showed a moderate inflammatory reaction as indicated by a score of 0.60 ± 0.24 . During the sixth week, the inflammatory response decreased, as indicated by scores of 2.40 ± 0.24 . During the twelfth-week observation, the inflammatory response is further decreased, as indicated by a score of 2.60 ± 0.24 .

On evaluation of the inflammatory reaction, it could be inferred that, although graft evoked an initial inflammatory response, it was minimal and subsided over time, becoming negligible.

4.4.1.2. Vascularity

In the early healing phase, group demonstrated abundant neovascularisation. However, vascularity progressively declined in the group from week two through week twelve. The scores for vascular response are presented in the Table 1.

4.4.1.3. Fibrosis

During the second week, the control defects showed moderate to marked fibrous tissue proliferation (1.40 ± 0.40). this fibrous proliferation was observed throughout the 12 weeks of observation.

4.4.1.4. New Bone Amount and Type

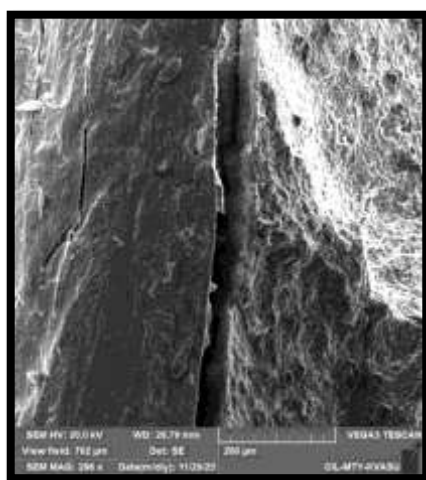
At week 2, the group exhibited small islands of woven bone within the defect area near its periphery. By week 12, the defect (score 2.00 ± 0.32) demonstrated a mixture of woven and mature lamellar bone arranged in thin layers extending from the cortical edges into the defect. The group showed a transition from woven bone to mature lamellar bone between the second and twelfth weeks.

4.4.1.5. Edge bone Integration

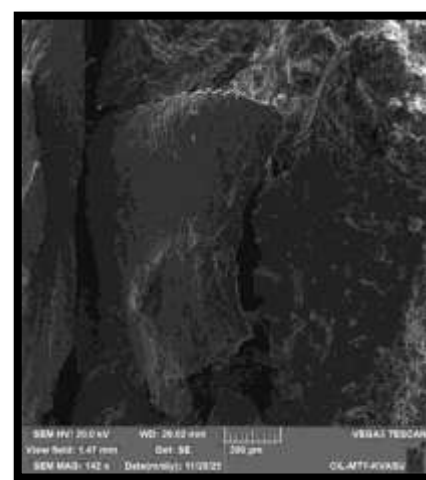
At two weeks, the group demonstrated edge bone integration, with a score of 1.40 ± 0.60 . By the sixth and twelfth weeks, the group continued to show edge integration, following a similar pattern of healing as the defect matured.

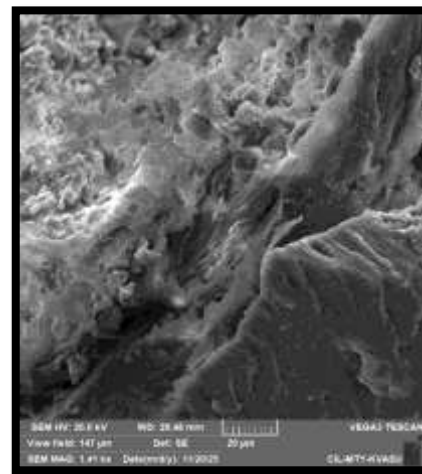
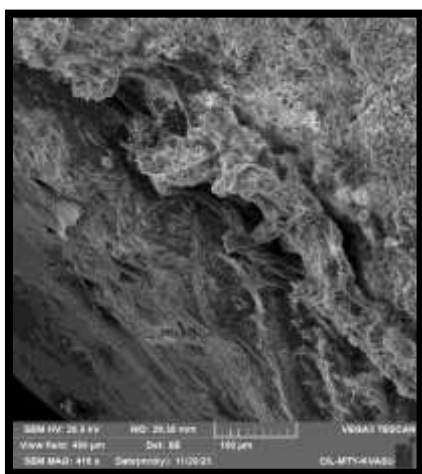
4.5. SCANNING ELECTRON MICROSCOPY

The specimens were examined using scanning electron microscopy to evaluate interfacial interactions, structural integration, and microarchitectural changes in the implanted grafts at sequential healing intervals. Retrieved samples at marked time points were assessed *via* SEM to visualise the morphology of the graft–host bone interface.

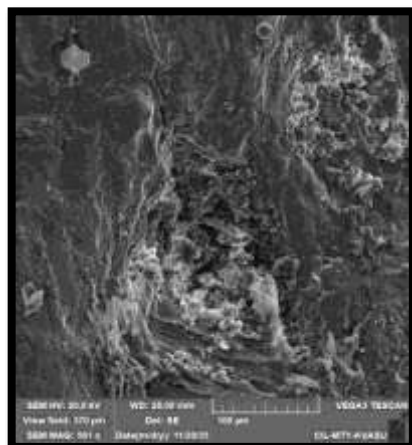
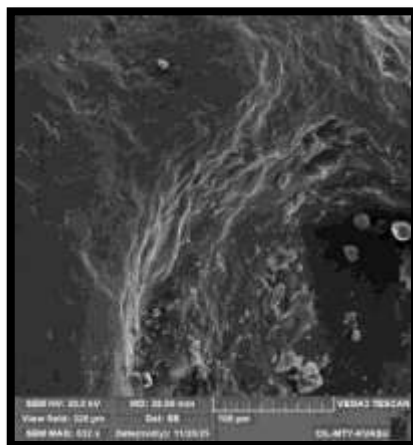


2nd week





6th week



12th week

Low-magnification SEM images enabled evaluation of overall graft incorporation, including the presence or resolution of interfacial gaps, surface continuity, and integration patterns. Higher magnifications provided detailed visualisation of cellular impressions, mineral deposition, and early osteoid formation.

At earlier time points, 2 weeks, there is a lack of tissue continuity and observable gaps between the graft material & the bone.

At the 6-week time point, there is considerable improvement in the group with bridging of the defect by cellular and extracellular matrix structures. The SEM shows initiation of lacunae like structure with remnants of graft.

At 12 weeks, the material exhibited a bridging behaviour with further integration into surrounding tissues. An extended time period ensures complete re-organisation of the tissue surrounding the test material. Some remnants of graft material may be present as discrete particulate matter that is visualised. The ongoing bio-degradation and remodelling in a controlled cascade are indicative of a controlled reparative healing cascade. The efficient healing and organised integration mediated by the elution of magnesium ions has been validated.

Overall, SEM analysis provided critical insight into graft performance by enabling direct visualisation of integration quality, biomaterial degradation, and microstructural features of newly formed bone.

5. DISCUSSION

Extensive bone defects—such as those resulting from comminuted fractures, tumour resections, or cystic lesions—often require surgical intervention with grafting materials to restore anatomical continuity and mechanical stability. Bone cements have become widely utilised in orthopaedic applications due to their mouldability, ease of handling, and ability to fill irregular defects. Magnesium phosphate cement (MPC) has gained increasing attention as an alternative to conventional calcium phosphate cements because of its relatively rapid setting time, superior compressive strength, and favourable biodegradation rate, as demonstrated by Tian et al. (2024).

In vitro studies indicate that MPC enhances osteoblastic proliferation and differentiation due to the sustained release of magnesium ions, which promote apatite deposition and interaction with serum proteins (Gelli & Ridi, 2023). Despite these advantages, MPC still presents limitations such as moderate mechanical strength and variable resorption kinetics, which necessitate further evaluation. Thus, the present study aimed to investigate the healing behaviour of a unicortical femoral defect filled with MPC and to characterise the radiographic, histological, histomorphometric, and microarchitectural outcomes of MPC-mediated bone regeneration in a rat model.

5.1 Selection and Evaluation of Experimental Animals

Male Wistar rats were selected for this study due to their consistent physiology, manageable size, and well-documented use in bone regeneration models. Their use aligns with recommendations by Mills and Simpson (2012), who noted that female reproductive hormonal fluctuations could influence bone healing parameters.

The surgically created 2×6 mm unicortical defect was positioned at the cranial aspect of the femoral diaphysis, similar to the approach described by Yang et al. (2024), taking advantage of the cylindrical anatomy of the bone which supports graft retention and stabilisation. All animals tolerated the surgical procedure well, with appropriate post-operative recovery and no wound complications, consistent with observations reported by Dinesh (2018) and Navya (2024).

5.4 Histological Evaluation

Histopathological analysis revealed time-dependent bone formation with MPC, with characteristic transitions from inflammation to woven bone formation and ultimately lamellar bone maturation.

Early Phase (2 Weeks)

MPC-treated defects exhibited moderate inflammatory cell infiltration and fibrous tissue within the defect area. Woven bone formation was initiated from the cortex to the defect site. These findings indicate that MPC launches an osteoconductive process but requires time for complete cellular infiltration and mineralisation.

Masson's trichrome staining showed predominance of collagen-rich fibrous tissue at this stage, correlating with early reparative activity described by Qiu et al. (2007).

Intermediate Phase (6 Weeks)

By six weeks, defects showed advanced bone deposition, thicker trabeculae, and improved continuity with host bone. Woven bone and early lamellar bone coexisted, demonstrating active remodelling. These observations agree with Yu et al. (2010) and Acarturk et al. (2008), who reported similar osteoconductive patterns in magnesium-based biomaterials.

Late Phase (12 Weeks)

By twelve weeks, the defect was largely filled with organised lamellar bone, although a small central gap covered by thin fibrous tissue remained in some samples. Osteoid deposition was pronounced, and the overall architecture suggested near-complete bone maturation. These results are consistent with Rentsch et al. (2014) and Dinesh (2018), who noted that MPC encourages steady maturation but may not fully close defects by this time without additional biological enhancement.

5.4.1 Histomorphometric Evaluation

Histomorphometric analysis further validated the histological observations.

- **Inflammation:** Moderate at two weeks, markedly reduced by six weeks, and minimal by twelve weeks—consistent with good material biocompatibility.
- **Neovascularisation:** Evident early and gradually declined, aligning with normal healing progression (Qiu et al., 2007).
- **Fibrosis:** Present initially and persisted to a mild degree throughout the healing period.
- **New Bone Formation:** Increased steadily from woven bone at two weeks to predominantly lamellar bone by twelve weeks.

- **Integration:** Enhanced edge bone formation indicated successful osteoconduction and graft incorporation.

These quantitative findings reflect MPC's ability to create a microenvironment conducive to neo-osteogenesis, although maturation is slower compared to highly bioactive graft composites described in other literature.

5.5 Scanning Electron Microscopy

SEM allowed high-resolution evaluation of the MPC–bone interface throughout healing.

At two weeks, MPC showed interfacial gaps and limited early bone apposition, consistent with minimal early osteoid formation. This correlates with findings by Brueckner et al. (2019) demonstrating delayed early adaptation in pure MPC interfaces.

At six weeks, ECM deposition increased, partially filling interfacial spaces. Lacunar structures and mineralising fronts became apparent, reflecting active woven bone formation. These observations align with Shah et al. (2019) regarding SEM differentiation of woven and lamellar bone.

By twelve weeks, interface consolidation improved significantly, although some discontinuity and residual MPC particles remained. The microarchitecture displayed organised lamellar-like structures accompanying gradual MPC degradation—consistent with controlled biodegradation described by John et al. (2008).

In summary, the present study establishes that MPC:

- is biocompatible and supports progressive bone regeneration,
- demonstrates early osteoconduction but slower maturation,
- undergoes controlled biodegradation over time,
- promotes stable graft–bone union by 12 weeks,
- but may leave residual material undergoing slow remodelling.

These characteristics reinforce MPC's usefulness as a clinically relevant bone cement, particularly in non-load-bearing or moderately load-bearing applications where gradual bone replacement is desired.

6. CONCLUSION

This study confirms that magnesium phosphate cement is an effective bone graft substitute capable of supporting progressive and organised bone regeneration in unicortical diaphyseal defects. MPC demonstrated strong biocompatibility, promoted early mineral deposition and osteoid formation, and facilitated a gradual transition from woven to lamellar bone. The material integrated well with host cortical structures and underwent controlled biodegradation compatible with physiological bone remodelling. Although residual material persisted in some areas, MPC's overall performance indicates its suitability for small to moderate cortical defects. Future progress may involve optimising its mechanical and biological properties through material reinforcement, microarchitectural engineering, or incorporation of additional bioactive components to broaden its applications in load-bearing orthopaedic reconstruction.

REFERENCE

Acarturk, O., Lehmicke, M., Aberman, H., Toms, D., Hollinger, J. O. and Fulmer, M. (2008). Bone healing response to an injectable calcium phosphate cement with enhanced radiopacity. *Journal of Biomedical Materials Research Part B: Applied Biomaterials: An Official Journal of The Society for Biomaterials, The Japanese Society for Biomaterials, and The Australian Society for Biomaterials and the Korean Society for Biomaterials*, 86(1), 56-62. <https://doi.org/10.1002/jbm.b.30987>

Brueckner, T., Heilig, P., Jordan, M. C., Paul, M. M., Blunk, T., Meffert, R. H. and Hoelscher-Doht, S. (2019). Biomechanical evaluation of promising different bone substitutes in a clinically relevant test set-up. *Materials*, 12(9), 1364. <https://doi.org/10.3390/ma12091364>

Costa, C. M., Bernardes, G., Ely, J. B., & Porto, L. M. (2011). Proposal for access to the femur in rats. *International Journal of Biotechnology and Molecular Biology Research*, 2(4), 73-79.

Dinesh, A., Dinesh, P. T., Fernandez, F. B., Sooryadas, S., Pradeep, M., Anoop, S. and Verma, H. K. (2024). Radiographic observations on healing of critical size calvarial defects treated with polyvinyl alcohol-hydroxyapatite composite ceramic in rat models. <https://doi.org/10.22271/veterinary.2024.v9.i1q.1123>

Dinesh, P. T. (2018). Healing of Bone Defects Treated with Tri-Phasic Composite Bio-Ceramic in Rat Models (Doctoral dissertation, College of Veterinary and Animal Sciences, Pookode Wayanad).

Gelli, R. and Ridi, F. (2023). An overview of magnesium-phosphate-based cements as bone repair materials. *Journal of functional biomaterials*, 14(8), 424. <https://doi.org/10.3390/jfb14080424>

John, A., Nair, M. B., Varma, H. K., Bernhardt, A. and Gelinsky, M. (2008). Biodegradation and cytocompatibility studies of a triphasic ceramic-coated porous hydroxyapatite for bone substitute applications. *International Journal of Applied Ceramic Technology*, 5(1), 11-19. <https://doi.org/10.1111/j.1744-7402.2008.02191.x>

Manasa, M. (2022). *Healing of Bone Defects Treated with Decellularised Tissue Engineered Triphasic Composite Bioceramic in Rat Calvarial Defect Model* (Doctoral Dissertation, College of Veterinary and Animal Sciences, Pookode, Wayanad, Kerala Veterinary and Animal Sciences University).

Mills, L. A. and Simpson, A. H. R. W. (2012). In vivo models of bone repair. *The Journal of Bone and Joint Surgery British Volume*, 94(7), 865-874. doi:10.1302/0301-620X.94B7.27370

Nair, M. B., Varma, H. K., Menon, K. V., Shenoy, S. J. and John, A. (2009). Reconstruction of goat femur segmental defects using triphasic ceramic-coated hydroxyapatite in combination with autologous cells and platelet-rich plasma. *Acta Biomaterialia*, 5(5), 1742-1755. <https://doi.org/10.1016/j.actbio.2009.01.009>

Navya P. S. (2024). Biomimetic Periosteal Membrane and Graft Filler for the Repair of Critical Size Femoral Defect In Rat Model. Doctoral dissertation, College of Veterinary and Animal Sciencs, Pookode, Wayanad, Kerala Veterinary and Animal Sciences University).

Qiu, Q. Q., Mendenhall, H. V., Garlick, D. S. and Connor, J. (2007). Evaluation of bone regeneration at critical-sized calvarial defect by DBM/AM composite. *Journal of Biomedical Materials Research Part B: Applied Biomaterials: An Official Journal of The Society for Biomaterials, The Japanese Society for Biomaterials, and The Australian Society for Biomaterials and the Korean Society for Biomaterials*, 81(2), 516-523. <https://doi.org/10.1002/jbm.b.30692>

Roberts, T. T. and Rosenbaum, A. J. (2012). Bone grafts, bone substitutes and orthobiologics: the bridge between basic science and clinical advancements in fracture healing. *Organogenesis*, 8(4), 114-124. <https://doi.org/10.4161/org.23306>

Tian, Y., Sun, R., Li, Y., Liu, P., Fan, B. and Xue, Y. (2024). Research progress on the application of magnesium phosphate bone cement in bone defect repair: a review. *Bio-Medical Materials and Engineering*, 35(3), 265-278. <https://doi.org/10.3233/BME-230164>

Yang, Q., Xu, M., Fang, H., Gao, Y., Zhu, D., Wang, J. and Chen, Y. (2024). Targeting micromotion for mimicking natural bone healing by using NIPAM/Nb2C hydrogel. *Bioactive Materials*, 39, 41-58. <https://doi.org/10.1016/j.bioactmat.2024.05.023>

Yu, Y., Wang, J., Liu, C., Zhang, B., Chen, H., Guo, H. and Huang, H. (2010). Evaluation of inherent toxicology and biocompatibility of magnesium phosphate bone cement. *Colloids and Surfaces B: Biointerfaces*, 76(2), 496-504. <https://doi.org/10.1016/j.colsurfb.2009.12.010>